

LM-MCVT: A Lightweight Multi-modal Multi-view Convolutional-Vision Transformer Approach for 3D Object Recognition

Songsong Xiong¹, Hamidreza Kasaei¹

Abstract—In human-centered environments such as restaurants, homes, and warehouses, robots often face challenges in accurately recognizing 3D objects. These challenges stem from the complexity and variability of these environments, including diverse object shapes. In this paper, we propose a novel Lightweight Multi-modal Multi-view Convolutional-Vision Transformer network (LM-MCVT) to enhance 3D object recognition in robotic applications. Our approach leverages the Globally Entropy-based Embeddings Fusion (GEEF) method to integrate multi-views efficiently. The LM-MCVT architecture incorporates pre- and mid-level convolutional encoders and local and global transformers to enhance feature extraction and recognition accuracy. We evaluate our method on the synthetic ModelNet40 dataset and achieve a recognition accuracy of 95.6% using a four-view setup, surpassing existing state-of-the-art methods. To further validate its effectiveness, we conduct 5-fold cross-validation on the real-world OmniObject3D dataset using the same configuration. Results consistently show superior performance, demonstrating the method’s robustness in 3D object recognition across synthetic and real-world 3D data.

I. INTRODUCTION

As societal growth accelerates, the increasing labor shortages are driving the integration of robots into human-centered environments such as homes, warehouses, and factories. These environments demand robots capable of performing tasks with efficient and accurate object recognition [1]. Effective object perception enables robots to understand, and safely interact with their surroundings. In recent years, advancements in three-dimensional (3D) object recognition technologies have significantly enhanced robots’ capabilities in perception, particularly in assistive and service-oriented robotic applications.

In general, 3D object recognition approaches can be categorized into three main categories: voxel-based, point-based, and view-based methods. Voxel-based methods [2]–[4] and point-based methods [5]–[8] use 3D meshes and point clouds, respectively. While these approaches comprehensively capture the spatial information of 3D objects, their high computational costs limit practicality [9]. In contrast, view-based methods enhance efficiency by converting 3D objects into 2D images from various viewpoints, simplifying the process and eliminating complex 3D feature processing [10]. For example, as shown in Fig. 1, a mug with rich features can be accurately recognized from multiple viewpoints. Benefiting from the advancement of deep learning, various methods encoded the rendered views to achieve a

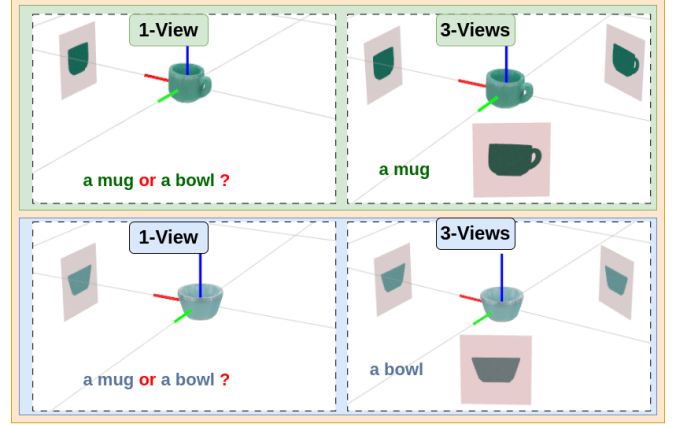


Fig. 1. An illustrative example of enhancing 3D object recognition by considering multiple viewpoints: In a single-view setup, different objects may look very similar and cannot be distinguished. In this example, the robot might be confused about whether the object is a *bowl* or *mug*. However, by considering more views of the object, the robot can observe specific features of the object and improve its recognition accuracy.

robust representation of a given object. For instance, [11]–[13] utilize 2D CNNs to extract features from multiple views of an object and aggregate these features for 3D object classification purposes. However, CNNs primarily focus on capturing local details while often overlooking global contextual relationships. Inspired by the ability of vision transformers to capture global spatial information, [14] introduced the multi-view vision transformer (MVT) for enhanced 3D object recognition. However, MVT relies on a simple average-pooling operation for view aggregation, which overlooks variations and unique contributions among views. Furthermore, as the number of ViT encoders increases, the model’s ability to retain local features weakens, limiting its overall performance. Previous research on multi-view object recognition was mainly focused on dense multi-view techniques to achieve better accuracy. Increasing the number of views can, to some extent, improve recognition accuracy, but acquiring dense multi-view data in real-world applications is often constrained by computational and memory requirements. Additionally, single-view methods incorporating depth information have been introduced to enhance object representation for 3D object recognition [15]. Compared to dense multi-view approaches, these single-view methods offer better efficiency but still face limitations in stability and robustness [15].

To achieve robust and efficient 3D object recognition, we propose the Lightweight Multi-modal Multi-view Convolutional-Vision Transformer network (LM-MCVT), il-

¹Department of Artificial Intelligence, University of Groningen, Groningen, The Netherlands
{s.xiong, hamidreza.kasaei}@rug.nl

illustrated in Fig. 2. We conduct extensive experiments, showing that our method surpasses state-of-the-art approaches in 3D object recognition performance. Furthermore, we deploy our model in real-world robotic scenarios for 3D object recognition and manipulation, demonstrating its robustness and reliability. In summary, our key contributions are twofold:

- We propose a Lightweight Multi-modal Multi-view Convolutional-Vision Transformer (LM-MCVT) network for 3D object recognition. Our approach integrates convolutional encoders and vision transformers to jointly capture local and global features, achieving superior performance with significantly reduced computational cost compared to existing methods.
- We develop the Globally Entropy-based Embeddings Fusion (GEEF) method, a novel feature aggregation strategy that leverages entropy-based weighting to adaptively fuse embeddings from multiple viewpoints. This approach efficiently integrates multi-modal multi-view representations, enhancing the performance of 3D object recognition.

II. RELATED WORK

In this section, we review the key efforts in 3D object recognition, focusing on voxel-based, point-based, and view-based methods.

Voxel-based methods: Such approaches represent an object’s point cloud data using discretized 3D voxel structures. For example, Maturana et al. [2] introduced the VoxNet framework for 3D object classification, utilizing an integrated volume-occupying grid representation with 3D CNNs. However, the performance of VoxNet is constrained by its resolution due to sparse data [16]. He et al. [4] combined spatial-filling curves with the octree structure to encode volumetric data. Although this approach reduces memory usage compared to voxel grids, it still requires significant memory for large-scale or high-resolution 3D data.

Point-based methods: These approaches use point cloud data directly. For instance, PointNet [5], a pioneering method, recognizes 3D objects by directly processing point cloud data. To enhance the performance of PointNet, MAP [7], a transformer-based approach, was developed to extract high-level latent features from unmasked point patches. Point cloud mamba was introduced to model point cloud data at a global level, further improving performance [8]. Compared to voxel-based methods, point-based approaches efficiently handle unstructured and irregularly sampled data, avoiding the need for uniform grids or meshes. However, accurate recognition in point-based methods still requires substantial computational resources, limiting their practical applicability [9].

View-based methods: These methods represent a 3D object by projecting it into multiple 2D images captured from various viewpoints. Our method belongs to this category. Hou et al. [17] used CNNs to encode multiple views, then applied reinforcement learning to select the next-best-view for 3D object recognition. Alzahrani et al. [12] employed

the most discriminative views of an object and achieved competitive accuracy in 3D object classification tasks. While these approaches have advanced the field, their reliance on heavy backbone networks often results in high memory usage and increased computational time, posing challenges for mobile devices. Moreover, such methods frequently prioritize extracting local features over capturing global spatial information [18]. Chen et al. [14] proposed the Multi-view Vision Transformer (MVT), a 3D object classification network that uses the middle-weight DeiT backbone. MVT incorporates multi-head attention to capture global object information and enables effective communication across different views through a unified global structure. However, as the number of layers in the MVT backbone increases, the focus on capturing local details from input views diminishes [18]. To further enhance 3D object recognition, Wang et al. proposed the optimal viewpoint pooling transformer, which obtains the best viewpoint settings from dense views to optimize performance [13]. In contrast to our approach, this method faces substantial challenges when optimal viewpoints are unavailable. Obtaining all views or dense views for a mobile robot in real-world scenarios, particularly in dynamic environments, presents practical difficulties.

Compared to the previous RGB-only methods, RGBD approaches demonstrate superior performance, especially when fewer views are available. For example, Kumra et al. [19] introduced a RGBD method to effectively guide robotic manipulation. Tzafas et al. [15] transferred pre-trained Vision Transformers to the RGBD domain for 3D object recognition by focusing on late-fusion cross-modal interactions at the downstream stage. Additionally, depth information was utilized to augment the 3D object detection [20]. Wang et al. [21] grouped multiple views with depth information into dominant sets and append the clustered vectors by recurrent cluster-pooling layer. Similar to our approach, [21] leveraged multiple RGBD views for object recognition, achieving improved accuracy compared to single-view methods. However, unlike our approach, its simplistic cluster-pooling strategy fails to effectively capture the unique characteristics of individual viewpoints. Moreover, the proposed method in [21] added a significant computational burden, ultimately limiting its overall recognition performance.

III. METHODOLOGY

An overview of the proposed approach is presented in Fig. 2. This section provides a detailed explanation of each building block.

A. Pre-Residual Convolutional Encoders

First, a 3D object is rendered into multiple views, where each view $v^j (j = 1, \dots, l)$ includes both RGB and depth images, as illustrated in Fig. 2. The resulting multi-modal RGBD data from these viewpoints are subsequently processed through convolutional layers, followed by normalization.

After initial processing, the views are fed into the pre-residual convolutional encoders. In the m -th pre-residual

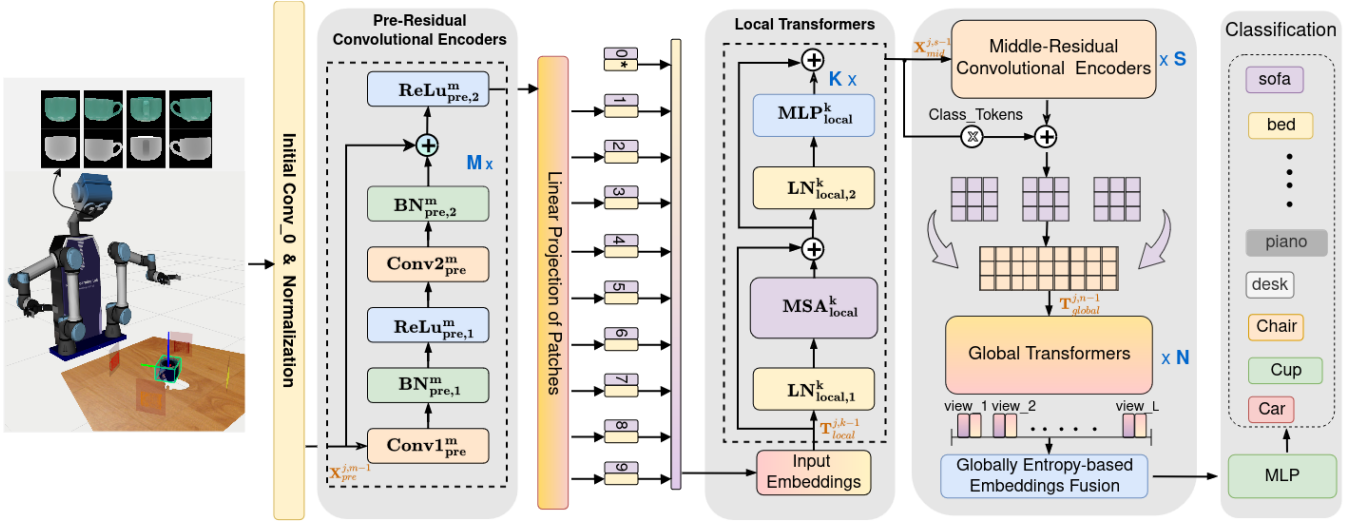


Fig. 2. LM-MCVT Framework for 3D Object Recognition in Robotic Perception. The 3D object, i.e., *a cup*, is projected onto RGB and Depth images from multiple viewpoints. After initial convolution and normalization, the multi-view representations are encoded using $M \times$ pre-residual convolutional encoders and projected into patches. These undergo global feature learning via $K \times$ local transformers and are refined through $S \times$ middle-residual encoders. Class token embeddings are combined with middle-residual output in $N \times$ global transformers. Finally, global entropy-based fusion integrates the multi-view representations for 3D object recognition.

convolutional stage, the input $\mathbf{X}_{pre}^{j,m-1}$ undergoes a sequential series of operations, including Conv1_{pre}^m , $\text{BN}_{pre,1}^m$, $\text{ReLU}_{pre,1}^m$, Conv2_{pre}^m , and $\text{BN}_{pre,2}^m$. Each convolutional operation employs a 3×3 kernel with a stride of 1 and padding of 1. To further enhance residual mapping, the resulting features are combined with $\mathbf{X}_{pre}^{j,m-1}$, followed by activation through $\text{ReLU}_{pre,2}^m$. The processed output is then passed on for subsequent feature extraction in the next stage.

B. Local Transformers

The local transformer network captures global properties by encoding the output of the pre-residual network. Initially, the output is divided into p patches, which are then projected into sequences of feature vectors, represented as $\mathbf{F} = [x_{p_1}^j, x_{p_2}^j, x_{p_3}^j, \dots, x_{p_w}^j]$. Here, $x_{p_w}^j \in \mathbb{R}^{192}$ denotes the feature projection of the p_w -th patch in the j -th view. To incorporate spatial information, a position sequence is added to the feature vectors based on the patch order, along with a *cls_token* that aggregates global patch information. This results in the input to the local transformer network, formulated as $\mathbf{T} = [x_{cls}, x_{p_1}, x_{p_2}, x_{p_3}, \dots, x_{p_w}] + \mathbf{E}_{pos}$, where $x_{cls} \in \mathbb{R}^{192}$ is a randomly initialized vector, and $\mathbf{E}_{pos} = [E_0, E_{p_1}, E_{p_2}, E_{p_3}, \dots, E_{p_w}] \in \mathbb{R}^{(p_w+1) \times 192}$ denotes the positional embeddings.

The projected embeddings from the pre-residual network, denoted as $\mathbf{T}_{local}^{j,k-1}$, serve as the input to the local transformer encoders. Each encoder block comprises Layer Normalization (LN), Multi-head Self-Attention (MSA), and a Multi-layer Perceptron (MLP). First, the input $\mathbf{T}_{local}^{j,k-1}$ undergoes normalization via $\text{LN}_{local,1}^k$ and is processed by MSA_{local}^k , producing an intermediate representation. Subsequently, the intermediate representation, combined with $\mathbf{T}_{local}^{j,k-1}$, is passed through $\text{LN}_{local,2}^k$ and MLP_{local}^k , followed by the addition of residual connections. The procedure of the k -th local

transformer block is illustrated in Fig. 2.

C. Middle-Residual Convolutional Encoders

The middle-residual convolutional network enhances local feature representations derived from transformer-encoded embeddings. As illustrated in Fig. 2, the transformer embeddings, excluding the *class_tokens*, are reshaped into feature maps and processed through a series of layers: Conv3_{mid}^s , $\text{BN}_{mid,1}^s$, $\text{ReLU}_{mid,1}^s$, Conv4_{mid}^s , $\text{BN}_{mid,2}^s$, and $\text{ReLU}_{mid,2}^s$.

In the s -th encoder of the middle-residual network, the input $\mathbf{X}_{mid}^{j,s-1}$ is first passed through Conv3_{mid}^s , followed by batch normalization $\text{BN}_{mid,1}^s$ and activation using $\text{ReLU}_{mid,1}^s$, producing an intermediate feature map $\mathbf{X}_{relu_1}^{j,s}$. This intermediate output is further processed by Conv4_{mid}^s and $\text{BN}_{mid,2}^s$, after which the residual input $\mathbf{X}_{mid}^{j,s-1}$ is added. And then the combined result is activated by $\text{ReLU}_{mid,2}^s$.

D. Global Transformers

The global transformer network is designed to collaboratively process embeddings from multiple views. The synthesized patch features, denoted as $\mathbf{T}_{global}^{j,n-1}$, are formed by combining the outputs of middle-residual convolutional blocks and the *class_tokens* from the local transformer network. This concatenated representation forms the input matrix for the global transformer.

In the n -th global transformer encoder, the input $\mathbf{T}_{global}^{j,n-1}$ is normalized by $\text{LN}_{global,1}^n$ and then processed by multi-head self-attention (MSA_{global}^n). The output of MSA_{global}^n is combined with the input $\mathbf{T}_{global}^{j,n-1}$ to produce $\mathbf{T}_{global,1}^{j,n}$. This intermediate result is further processed by $\text{LN}_{global,2}^n$ and a multi-layer perceptron (MLP_{global}^n), with the output combined with $\mathbf{T}_{global,1}^{j,n}$ to generate $\mathbf{T}_{global}^{j,n}$, the input for the next stage.

E. Globally Entropy-based Embeddings Fusion (GEEF)

After processing the input views using global transformers, the object embeddings are represented as $\mathbf{T}_v = [\mathbf{t}_{v_1}, \mathbf{t}_{v_2}, \dots, \mathbf{t}_{v_j}, \dots, \mathbf{t}_{v_l}]$. These extracted representations are then fused and processed through an MLP for object classification. Previous fusion methods commonly use average pooling and max pooling to merge all representations. However, these methods overlook the unique contributions and feature discrepancies across different views, resulting in inadequate fusion of multi-view representations. Moreover, classification embeddings from transformer blocks primarily depend on a single class token, which inadequately captures comprehensive spatial information. To mitigate these limitations, we propose a global entropy-based embedding fusion method to effectively integrate multi-view representations. We begin by applying average pooling to fuse the embeddings of RGB views, denoted as $\mathbf{E}_v^{rgb} = [\mathbf{e}_{v_1}, \mathbf{e}_{v_2}, \dots, \mathbf{e}_{v_j}, \dots, \mathbf{e}_{v_l}]$, while excluding the class tokens, to obtain the fused representation \mathbf{E}^{RGB} .

Next, the entropy of the RGB representation, denoted as $H_v^{cls}(c_{v_j}) = -\sum_{j=1}^l p_{c_{v_j}} \log p_{c_{v_j}}$, is computed from the class token vectors across all RGB views, aggregated in $\mathbf{C}_v^{rgb} = [\mathbf{c}_{v_1}, \mathbf{c}_{v_2}, \dots, \mathbf{c}_{v_j}, \dots, \mathbf{c}_{v_l}]$. To utilize entropy values for feature fusion, they need to be normalized to obtain the weights w_{v_j} for each view. The normalization formula is as follows:

$$w_{v_j} = \frac{H_v^{cls}(c_{v_j})}{\sum_{j=1}^l H_v^{cls}(c_{v_j})} \quad (1)$$

where w_{v_j} represents the weight of the j -th view. Based on the entropy weights w_{v_j} , a fusion operation of *class_tokens* is performed on the features from each view. The final fused *class_tokens* \mathbf{C}^{RGB} is expressed as:

$$\mathbf{C}^{RGB} = \sum_{j=1}^l w_{v_j} \mathbf{c}_{v_j} \quad (2)$$

Similarly, we compute the corresponding fused depth features, denoted as \mathbf{E}^{Depth} and \mathbf{C}^{depth} . To enhance the representation capability for final classification, a concatenation is applied to aggregate all the representations.

IV. EXPERIMENTS

This section summarizes the implementation details and comprehensively evaluates our approach. We analyzed fused-embedding methods, investigated pre- and middle-residual convolutional encoders to determine the optimal LM-MCVT structure, and conducted ablation studies comparing transformers and convolutional encoders. The method's performance and robustness were assessed under varying numbers of views and view structures from multi-modal data. Finally, we compared our results with state-of-the-art methods under consistent viewpoint configurations.

A. Implementation Details

We used two datasets: the synthetic ModelNet dataset [22] and the real-world OmniObject3D dataset [23]. For the offline experiments on ModelNet, which includes ModelNet10

TABLE I
ACCURACY (%) OF DIFFERENT FUSED EMBEDDING METHODS

Inputs	Fusion Embedding Methods			
	ACF	ECF	AEF	GEEF
RGB	94.1	93.8	93.2	94.4
RGBD	94.3	94.4	95.4	96.6

and ModelNet40, we evaluated our model using the training and testing splits outlined in [14]. ModelNet40 contains 12311 3D CAD models across 40 categories, with 9843 models for training and 2468 for testing. ModelNet10 is a 10-category subset. OmniObject3D is a large-scale dataset of high-quality, real-scanned 3D objects, featuring 6000 objects across 190 everyday categories. For OmniObject3D, we adopted the same view settings as ModelNet. To evaluate our approach, we employed a 5-fold cross-validation strategy, which provides a robust estimate of the model's performance and minimizes the risk of overfitting to specific subsets. We conducted our experiments using an NVIDIA V100 graphics card. Our approach was trained with the Adam optimizer, starting with a learning rate of 0.0002 and betas set to [0.9, 0.98]. To optimize training, we dynamically adjusted the learning rate using a cosine annealing schedule.

B. Performance Analysis of Fusion Strategies

Our initial experiments explored multi-view fusion techniques. In vision transformer architectures, class token embeddings are commonly used for classification tasks [24]. However, incorporating embeddings beyond the *class_tokens* contributes to enhancing the final object representation [18]. Building on these findings, we proposed the globally entropy-based embedding fusion method (GEEF) and conducted experiments to compare its performance with other fusion techniques.

- *Average-pooling-based Class_tokens Fusion (ACF)*: This fusion methodology primarily centers on the averaging of class tokens extracted from multiple views [14].
- *Entropy-based Class_tokens Fusion (ECF)*: ECF fuses multi-view representations using entropy distinctions among class tokens from various views.
- *Average-pooling-based Embeddings Fusion (AEF)*: This fusion method utilizes average pooling to integrate multiple patch-based image embeddings without including class tokens.

To evaluate the effectiveness of GEEF, we conducted 3D object classification experiments on the ModelNet10 dataset. Each object was observed from three different viewpoints with equal interval angles. For a fair comparison, we used the LM-MCVT network, excluding the pre- and middle-residual convolutional encoders.

The experimental results in Table I highlight the superiority of our proposed GEEF method compared to other fusion embedding techniques. GEEF consistently achieves higher accuracy for both RGB and RGBD inputs, outperforming the next-best method (AEF) by up to 1.2% in the RGBD setting.

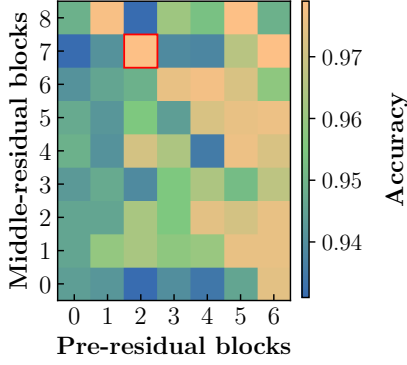


Fig. 3. Ablation study on the effects of pre-residual and middle-residual block configurations on model accuracy.

This improvement can be attributed to GEEF’s ability to effectively capture and integrate information from multi-modal multi-view data, leading to a more robust and discriminative feature representation. These findings underscore GEEF’s effectiveness in leveraging multi-modal data for enhanced performance.

C. Ablation Study for Convolutional Encoders and Global Transformers

In this round of experiments, we utilized the ModelNet10 dataset to evaluate the model’s performance. We aimed to construct the LM-MCVT network by integrating residual convolutional and transformer encoders. Convolutional encoders excel at extracting local features, while Vision Transformers (ViT) are favored for capturing global information [18]. However, as the number of ViT layers increases, their capacity to capture local features diminishes [18]. To address this, we incorporated pre- and middle-residual convolutional layers into the LM-MCVT network to enhance the acquisition of local and global features. Inspired by [14], we employed a local-global structure to facilitate interaction across views. We set local transformers to 8 and global transformers to 4. We then extensively evaluated the impact of convolutional residual encoders. We analyzed the performance by separately removing pre- and middle-residual blocks and studied the effects of increasing both. The experimental results, illustrated in Fig. 3, demonstrate that configurations with more convolutional-residual blocks generally achieve better recognition performance. This improvement can be attributed to the enhanced capacity of residual blocks to learn hierarchical and complex feature representations. By mitigating the vanishing gradient problem, residual connections enable deeper networks to be trained effectively without performance degradation, facilitating better extraction and integration of multi-scale features essential for recognizing complex patterns. LM-MCVT achieves an optimal balance between accuracy and robustness with nine pre- and middle-residual blocks. To ensure a lightweight yet accurate model, we selected a configuration with two pre-residual blocks and seven middle-residual blocks, as shown in the red square of Fig. 3. This finalized network configuration will be used in subsequent experiments.

TABLE II
ABLATION STUDY ON THE IMPACT OF CONVOLUTIONAL ENCODERS AND TRANSFORMERS ON MODEL ACCURACY (%)
WITH MULTI-MODAL (RGB-D) DATA

Input	Without Pre_cnn	Without LT	Without Mid_cnn	Without GT	With All
RGBD	94.4	96.7	95.9	96.1	98.0

*LT refers to Local Transformers, and GT refers to Global Transformers.

To further investigate the impact of transformers and convolutional encoders on our model, we conducted an ablation study on each block using multi-modal (RGBD) data. The results, presented in Table II, emphasize the contributions of each component to the overall performance of LM-MCVT. The full configuration achieves the highest accuracy of 98.0%, highlighting the synergistic benefits of combining convolutional and transformer-based components. This integration leverages the strengths of both approaches, with convolutional encoders excelling at local feature extraction and transformers capturing long-range dependencies, ultimately leading to optimal performance.

D. Multi-Modal and Multi-View Analysis with Diverse Viewpoint Configurations

In this section, we present another round of experiments conducted on the ModelNet10 dataset to evaluate the performance of our approach. Multi-modal and multi-view experiments were performed using the viewpoint settings outlined in [14]. The results, summarized in Table III, show that recognition accuracy improves with an increasing number of views but comes at the cost of higher computation time per instance. A four-view configuration was found to offer the optimal balance between accuracy and computational efficiency. While dense views provide more detailed 3D object descriptions, they significantly increase recognition time, making them impractical for real-robot scenarios where computational constraints often limit the number of views robots can capture. This highlights the importance of efficient view selection for balancing performance and practicality.

In the second phase of our experiments, we evaluated the performance of our method across different structural arrangements of four viewpoints. Towards this goal, five cases of four-view configurations were randomly selected on a circular plane, as illustrated in Fig. 4. The results, summarized in Table IV, demonstrate that our method

TABLE III
PERFORMANCE OF LM-MCVT ON THE MODELNET10 DATASET WITH DIFFERENT NUMBERS OF VIEWS

Inputs	Metric	Different Number of Views					
		1	2	3	4	6	12
RGB	ACC (%)	93.2	95.3	97.8	98.2	97.7	98.1
	Time (ms)	1.3	1.7	2.4	3.3	5.1	12.0
RGBD	ACC (%)	95.5	97.2	98.0	98.5	98.1	98.9
	Time (ms)	1.7	3.2	5.1	7.0	11.6	29.7

*ACC refers to accuracy, and Time refers to the testing time per instance.

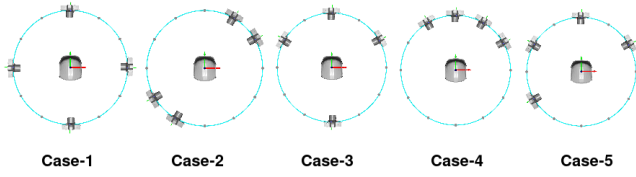


Fig. 4. Visualization of five cases of four-view structures with circular view-points for the object (*chair*) in ModelNet10.

TABLE IV

ACCURACY (%) OF DIFFERENT CIRCULAR FOUR-VIEW STRUCTURES ON MODELNET10 DATASET

Inputs	Circular four-view structures				
	case-1	case-2	case-3	case-4	case-5
RGB	98.2	95.2	97.1	96.9	96.2
RGBD	98.5	96.7	98.2	96.9	96.7

achieved consistent and reliable performance under diverse viewpoint configurations. This robustness can be attributed to the method’s ability to effectively integrate multi-view information and extract complementary features from different perspectives, ensuring accurate recognition even under varying structural setups.

Furthermore, we evaluated the performance of our method using four randomly selected viewpoints from hemidodecahedron structures. The configurations of these hemidodecahedron structures are illustrated in Fig. 5, and the corresponding results are presented in Table V. These results showed the robustness and effectiveness of our method in handling diverse spatial arrangements. The consistent accuracy across different cases highlights the method’s ability to efficiently integrate information from different viewpoints, ensuring reliable performance in 3D recognition tasks.

E. Comparison with State-of-the-art Methods

1) *Performance on ModelNet Dataset:* As summarized in Table VI, voxel-based methods, such as 3DShapeNet and VoxNet, show limited performance, achieving a maximum accuracy of 92.0% on ModelNet10 and 83.0% on ModelNet40. These approaches struggle with computational efficiency and resolution loss due to the voxelization process,

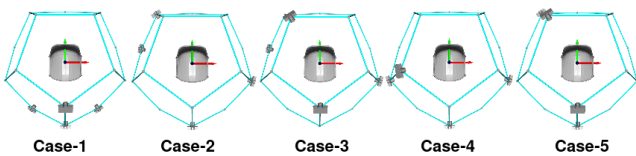


Fig. 5. Visualization of five cases of four-view structures with hemidodecahedron for the object (*chair*) in ModelNet10.

TABLE V

ACCURACY (%) OF DIFFERENT HEMI-DODECAHEDRON FOUR-VIEW STRUCTURES ON MODELNET10 DATASET

Inputs	Hemi-dodecahedron four-view structures				
	case-1	case-2	case-3	case-4	case-5
RGBD	98.2	99.1	99.2	99.0	98.8

TABLE VI
PERFORMANCE COMPARISON ON MODELNET DATASET

Methods	Params	Views	Accuracy (%)	
			ModelNet10	ModelNet40
Voxel-based Approaches				
3DShapeNet [22]	-	-	83.5	77.3
VoxNet [2]	-	-	92.0	83.0
VSO [4]	-	-	84.0	72.6
Point-based Approaches				
PCNN [25]	8.1M	-	94.9	92.3
PoinTramba [6]	19.5M	-	-	92.9
VPC [26]	8.0M	-	93.4	88.2
PCM [8]	34.2M	-	-	93.4
View-based Approaches				
MVCNN [27]	103M	80	-	90.1
LSV [17]	103M	12	-	94.5
MVTN [28]	73.4M	12	-	92.9
MVT [14]	22.2M	12	95.3	94.4
TMTL [29]	24.0M	12	95.15	93.68
VGP [30]	11.83M	12	96.47	95.31
SMV [12]	60.2M	12	-	88.13
LM-MCVT (RGB)	10.5M	4	98.2	95.5
LM-MCVT (Depth)			94.1	91.9
LM-MCVT(RGBD)			98.5	95.6

which limits their ability to capture fine-grained details of 3D objects. Point-based methods like PoinTramba and PCNN outperform voxel-based methods by directly operating on point clouds, achieving up to 94.9% accuracy on ModelNet10. However, these methods still fall short compared to view-based approaches due to challenges in efficiently capturing global and contextual features from sparse point clouds. View-based methods consistently outperform voxel-based and point-based techniques, leveraging multiple 2D projections to better preserve object details and contextual relationships. Among these, MVCNN achieves good accuracy but at the cost of significantly increased computational requirements due to the use of dense multi-view setups. Our method, LM-MCVT, achieves the best performance while maintaining computational efficiency. Specifically, on ModelNet10, LM-MCVT achieves 98.5% accuracy using only four views, outperforming heavier methods such as MVCNN, which requires 80 views, and lightweight approaches such as MVT and TMTL, which use 12 views. On ModelNet40, our method reaches an accuracy of 95.6%, demonstrating its robustness across datasets. Our method sets a new benchmark in terms of accuracy and efficiency. In particular, by effectively combining RGB and depth information, LM-MCVT leverages complementary features from both modalities, providing a richer representation of 3D objects. Furthermore, despite using only 10.5M parameters and four views, our method achieves state-of-the-art performance, offering a practical solution for real-world applications where computational resources and viewpoints are often limited. We attributed these results to the point that LM-MCVT extracted both local and global features through its convolutional and transformer-based architecture, allowing it to outperform methods with significantly more parameters or views.

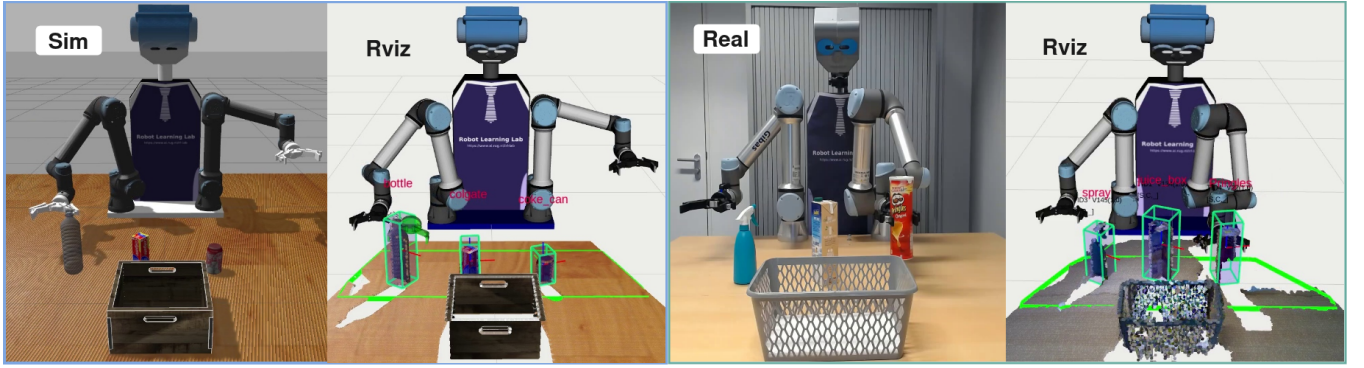


Fig. 6. The snapshots demonstrating the recognition performance of our dual-arm robot employing the LM-MCVT model in *pick_and_place* scenario: (Sim/Real) We randomly put three objects in the operational area of the robot. (Rviz) The robot is required to successfully recognize these objects using our fine-tuned 4-views LM-MCVT model, before manipulating them. Finally, the robot picked up objects and placed them into the basket.

TABLE VII
PERFORMANCE COMPARISON ON OMNIObject3D DATASET

Methods	Input	Params	Accuracy (%)	Time (ms)
MVT [14] (2021)	RGB	22.2M	60.74	6.5
	Depth		62.13	6.5
	RGBD		70.72	13.3
SMV [12] (2024)	RGB	60.2M	76.16	23.6
	Depth		69.50	23.6
	RGBD		81.02	64.3
LM-MCVT (Ours)	RGB	10.5M	83.33	3.3
	Depth		78.80	3.3
	RGBD		85.10	7.0

2) *Performance on OmniObject3D Dataset:* In this round of experiments, we conducted 5-fold cross-validation using four views. Since there are no established baselines for the OmniObject3D dataset, we trained all multi-view methods from scratch. The experimental results, presented in Table VII, demonstrate the performance of various methods on this challenging dataset. The OmniObject3D dataset is significantly more complex than ModelNet40. This increased complexity resulted in a performance drop across all methods compared to the ModelNet40 experiments. Despite this, our method, LM-MCVT, achieved a remarkable accuracy of 85.1%, outperforming the competing approaches. Specifically, LM-MCVT demonstrated superior performance across all input modalities (RGB, Depth, and RGBD), with its RGBD accuracy significantly surpassing that of SMV (81.0%) and MVT (70.7%). In addition to its accuracy, LM-MCVT proved to be highly computationally efficient. With an inference time of only 7.0 ms for RGBD inputs, it outperformed MVT (13.3 ms) and SMV (64.3 ms) while utilizing much fewer parameters (10.5M compared to 22.2M for MVT and 60.2M for SMV). This efficiency highlights the lightweight nature of our method, making it suitable for real-time applications. Moreover, LM-MCVT effectively leverages multi-modal data, maintaining high accuracy across different input types. This capability is particularly advantageous for the OmniObject3D dataset, which has diverse object categories requiring robust feature integration.

F. Robotic Demonstrations

To evaluate our method in a robotic setting, we initially fine-tuned the pre-trained LM-MCVT model on the Synthetic Household Object dataset [31]. For each object, we captured four views. This fine-tuning was necessary because the objects are partially visible to the robot due to (self) occlusion. The LM-MCVT model was fine-tuned using a 5-fold cross-validation approach, achieving a recognition accuracy of 99.3% on Synthetic Household Objects. In the experiment, we randomly positioned three objects in front of the robot, as depicted in Fig. 6. The first step involved segmenting the object from the surrounding environment [32], [33]. The robot then captured four RGBD views of the segmented objects, as illustrated in Fig. 2. These views were fed into the fine-tuned LM-MCVT model to identify the object. Subsequently, the robot detected a suitable grasp configuration for each target object, grasping and relocating them into a basket [34]. The process is detailed in Fig. 6, which shows the performance of the robot in sim-real settings and the visualization of recognition in RViz. We conducted ten rounds of experiments. Across all trials, the robot consistently identified, picked up, and placed the objects correctly, demonstrating the robustness and reliability of the LM-MCVT model in handling real-world variations. The success of these experiments underscores the practical applicability of our model in real-robot settings.

V. CONCLUSION

In this study, we introduced the Lightweight Multi-Modal Multi-View Convolutional-Vision Transformer (LM-MCVT) network, an innovative framework designed to enhance 3D object recognition in various real-world applications. Our approach integrates convolutional encoders and transformers to effectively extract and fuse multi-modal, multi-view data. A key contribution of our work is the introduction of the Globally Entropy-based Embeddings Fusion (GEEF) method, which optimally combines information from different views to improve recognition accuracy. Through a series of comprehensive experiments, we demonstrated the superiority of the LM-MCVT network in comparison to existing state-of-the-art methods. Notably, our model achieved

state-of-the-art performance on both synthetic and real-world datasets, including the ModelNet and OmniObject3D datasets. Specifically, the LM-MCVT network exhibited superior accuracy while maintaining a lightweight architecture, making it suitable for deployment in environments with computational constraints. Moreover, the integration of the LM-MCVT model into a dual-arm robotic framework highlighted its practical applicability. The robot was able to accurately recognize and manipulate objects, demonstrating the model's robustness and effectiveness. In the continuation of this work, inspired by the advancements in large vision-language models (VLMs), such as those demonstrated in [35], we plan to investigate a hybrid approach that combines geometric and visual information with the contextual reasoning capabilities of VLMs.

ACKNOWLEDGMENT

We thank the Center for Information Technology of the University of Groningen for their support and for providing access to the high performance computing cluster - Hábrók.

REFERENCES

- [1] G. Liu, Y. Hu, Z. Chen, J. Guo, and P. Ni, "Lightweight object detection algorithm for robots with improved yolov5," *Engineering Applications of Artificial Intelligence*, vol. 123, p. 106217, 2023.
- [2] D. Maturana and S. Scherer, "Voxnet: A 3d convolutional neural network for real-time object recognition," in *2015 IEEE/RSJ international conference on intelligent robots and systems (IROS)*. IEEE, 2015, pp. 922–928.
- [3] O. V. Putra, M. I. Riansyah, A. Priyadi, E. M. Yuniarno, M. H. Purnomo *et al.*, "Fuzzy lightweight cnn for point cloud object classification based on voxel," in *TENCON 2023-2023 IEEE Region 10 Conference (TENCON)*. IEEE, 2023, pp. 685–690.
- [4] Z. He, X. Liu, and C. Zhang, "Similarity measurement and retrieval of three-dimensional voxel model based on symbolic operator," *ISPRS International Journal of Geo-Information*, vol. 13, no. 3, p. 89, 2024.
- [5] C. R. Qi, H. Su, K. Mo, and L. J. Guibas, "Pointnet: Deep learning on point sets for 3d classification and segmentation," in *Proceedings of the IEEE conference on computer vision and pattern recognition*, 2017, pp. 652–660.
- [6] Z. Wang, Z. Chen, Y. Wu, Z. Zhao, L. Zhou, and D. Xu, "Pointtramba: A hybrid transformer-mamba framework for point cloud analysis," *arXiv preprint arXiv:2405.15463*, 2024.
- [7] Y. Pang, W. Wang, F. E. Tay, W. Liu, Y. Tian, and L. Yuan, "Masked autoencoders for point cloud self-supervised learning," in *European conference on computer vision*. Springer, 2022, pp. 604–621.
- [8] T. Zhang, X. Li, H. Yuan, S. Ji, and S. Yan, "Point could mamba: Point cloud learning via state space model," *arXiv preprint arXiv:2403.00762*, 2024.
- [9] H.-Y. Zhou, A.-A. Liu, W.-Z. Nie, and J. Nie, "Multi-view saliency guided deep neural network for 3-d object retrieval and classification," *IEEE Transactions on Multimedia*, vol. 22, no. 6, pp. 1496–1506, 2019.
- [10] S. Qi, X. Ning, G. Yang, L. Zhang, P. Long, W. Cai, and W. Li, "Review of multi-view 3d object recognition methods based on deep learning," *Displays*, vol. 69, p. 102053, 2021.
- [11] H. Kasaei, M. Kasaei, G. Tzifas, S. Luo, and R. Sasso, "Simultaneous multi-view object recognition and grasping in open-ended domains," *Journal of Intelligent & Robotic Systems*, vol. 110, no. 2, pp. 1–19, 2024.
- [12] M. Alzahrani, M. Usman, S. Anwar, and T. Helmy, "Selective multi-view deep model for 3d object classification," in *Proceedings of the IEEE/CVF Conference on Computer Vision and Pattern Recognition (CVPR) Workshops*, June 2024, pp. 728–736.
- [13] W. Wang, G. Chen, H. Zhou, and X. Wang, "Ovpt: Optimal viewset pooling transformer for 3d object recognition," in *Proceedings of the Asian Conference on Computer Vision*, 2022, pp. 4444–4461.
- [14] S. Chen, T. Yu, and P. Li, "MVT: multi-view vision transformer for 3d object recognition," in *BMVC*, 2021.
- [15] G. Tzifas and H. Kasaei, "Early or late fusion matters: Efficient rgb-d fusion in vision transformers for 3d object recognition," in *2023 IEEE/RSJ International Conference on Intelligent Robots and Systems (IROS)*. IEEE, 2023, pp. 9558–9565.
- [16] W. Wang, T. Wang, and Y. Cai, "Multi-view attention-convolution pooling network for 3d point cloud classification," *Applied Intelligence*, vol. 52, no. 13, pp. 14787–14798, 2022.
- [17] Y. Hou, S. Gould, and L. Zheng, "Learning to select views for efficient multi-view understanding," in *Proceedings of the IEEE/CVF Conference on Computer Vision and Pattern Recognition*, 2024, pp. 20135–20144.
- [18] M. Raghu, T. Unterthiner, S. Kornblith, C. Zhang, and A. Dosovitskiy, "Do vision transformers see like convolutional neural networks?" *Advances in Neural Information Processing Systems*, vol. 34, pp. 12116–12128, 2021.
- [19] S. Kumra, S. Joshi, and F. Sahin, "Antipodal robotic grasping using generative residual convolutional neural network," in *2020 IEEE/RSJ International Conference on Intelligent Robots and Systems (IROS)*. IEEE, 2020, pp. 9626–9633.
- [20] J. Zhou, L. Wang, H. Lu, K. Huang, X. Shi, and B. Liu, "Mysalnet: Multi-view augmentation for rgb-d salient object detection," in *European Conference on Computer Vision*. Springer, 2022, pp. 270–287.
- [21] C. Wang, M. Pelillo, and K. Siddiqi, "Dominant set clustering and pooling for multi-view 3d object recognition," *arXiv preprint arXiv:1906.01592*, 2019.
- [22] Z. Wu, S. Song, A. Khosla, F. Yu, L. Zhang, X. Tang, and J. Xiao, "3d shapenets: A deep representation for volumetric shapes," in *Proceedings of the IEEE conference on computer vision and pattern recognition*, 2015, pp. 1912–1920.
- [23] T. Wu, J. Zhang, X. Fu, Y. Wang, J. Ren, L. Pan, W. Wu, L. Yang, J. Wang, C. Qian *et al.*, "Omniobject3d: Large-vocabulary 3d object dataset for realistic perception, reconstruction and generation," in *Proceedings of the IEEE/CVF Conference on Computer Vision and Pattern Recognition*, 2023, pp. 803–814.
- [24] A. Dosovitskiy, L. Beyer, A. Kolesnikov, D. Weissenborn, X. Zhai, T. Unterthiner, M. Dehghani, M. Minderer, G. Heigold, S. Gelly *et al.*, "An image is worth 16x16 words: Transformers for image recognition at scale," *arXiv preprint arXiv:2010.11929*, 2020.
- [25] M. Atzmon, H. Maron, and Y. Lipman, "Point convolutional neural networks by extension operators," *arXiv preprint arXiv:1803.10091*, 2018.
- [26] A. S. Gezawa, Z. A. Bello, Q. Wang, and L. Yunqi, "A voxelized point clouds representation for object classification and segmentation on 3d data," *The Journal of Supercomputing*, vol. 78, no. 1, pp. 1479–1500, 2022.
- [27] H. Su, S. Maji, E. Kalogerakis, and E. Learned-Miller, "Multi-view convolutional neural networks for 3d shape recognition," in *Proceedings of the IEEE international conference on computer vision*, 2015, pp. 945–953.
- [28] A. Hamdi, F. AlZahrani, S. Giancola, and B. Ghanem, "Mvtn: Learning multi-view transformations for 3d understanding," *International Journal of Computer Vision*, pp. 1–30, 2024.
- [29] Y. Zhang, S. Fu, and Y. Qu, "Tensor multi-task learning for multi-view representation of 3d shape," in *2023 China Automation Congress (CAC)*. IEEE, 2023, pp. 4703–4708.
- [30] L. Han, J. He, F. Dou, H. Ma, X. Xie, and W. Yang, "A viewpoint-guided prototype network for 3d shape classification," *Multimedia Systems*, vol. 29, no. 6, pp. 3531–3547, 2023.
- [31] H. Kasaei and S. Xiong, "Lifelong ensemble learning based on multiple representations for few-shot object recognition," *Robotics and Autonomous Systems*, vol. 174, p. 104615, 2024.
- [32] S. H. Kasaei, M. Oliveira, G. H. Lim, L. S. Lopes, and A. M. Tomé, "Towards lifelong assistive robotics: A tight coupling between object perception and manipulation," *Neurocomputing*, vol. 291, pp. 151–166, 2018.
- [33] S. H. Kasaei, "Orthographicnet: A deep transfer learning approach for 3-d object recognition in open-ended domains," *IEEE/ASME Transactions on Mechatronics*, vol. 26, no. 6, pp. 2910–2921, 2020.
- [34] H. Kasaei and M. Kasaei, "Mygrasp: Real-time multi-view 3d object grasping in highly cluttered environments," *Robotics and Autonomous Systems*, vol. 160, p. 104313, 2023.
- [35] G. Tzifas and H. Kasaei, "Towards open-world grasping with large vision-language models," in *8th Annual Conference on Robot Learning*, 2024.